

Position-Selective Metal Oxide Nanostructures using Atomic Thin Carbon Layer for Hydrogen Gas Sensors

Hak Ki Yu[†]

Abstract

A hydrogen sensor was fabricated by utilizing a bundle of metal oxide nanostructures whose growth positions were selectively controlled by utilizing graphene, which is a carbon of atomic-unit thickness. To verify the reducing ability of graphene, it was confirmed that the multi-composition metal oxide V_2O_5 was converted into VO_2 on the graphene surface. Because of the role of graphene as a reducing catalyst, it was confirmed that ZnO and MoO_3 nanostructures were grown at high density only on the graphene surface. The fabricated gas sensor showed excellent sensitivity.

Keywords: Metal oxide, Position selective growth, Atomic carbon layer, Hydrogen sensors

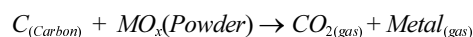
1. INTRODUCTION

The increased social/public interest in hydrogen as a future energy source has led to increasing demands for its safe use [1]. When hydrogen reaches a concentration of $\geq 4\%$ in the atmosphere, it reacts with oxygen and explodes; hence, the accurate monitoring of gaseous hydrogen in real time is very important. An optical-based sensor is mainly required for concentrations $\geq 4\%$, whereas at low ppb-level concentrations, an electronic sensor capable of detecting trace amounts is used [2,3]. In other words, the overall management of hydrogen concentration requires the simultaneous use of two types of sensors.

To detect very low concentrations of hydrogen, numerous studies have been conducted on an electronic sensor that utilizes the change in the resistance of a metal oxide (MO_x) semiconductor. Hydrogen removes the OH group adsorbed on the metal oxide and increases the electron concentration on the surface, which increases the electrical conductivity of n-type oxide semiconductors; the opposite is true for p-type semiconductors [4]. To increase the sensitivity of such a gas sensor, it is necessary to increase the surface area. Thus, research has been conducted to

fabricate various metal oxide nanostructures for application in hydrogen sensors [5-8]. In general, for a nanostructured hydrogen sensor, a unit device is fabricated by forming an electrode after separating the synthesized nanostructure. If the detection device is fabricated using a single nanorod, the complex fabrication process (such as e-beam lithography) leads to lower productivity and higher processing costs. An alternative method is to synthesize a bundle of connected nanostructures to form an electrode, and then fabricating the sensor with high sensitivity.

To apply such a bundle of nanostructures to a sensor, it is very important to have technology that can selectively grow nanostructures in a desired area. In this study, an atomic-unit-thick carbon layer (graphene) was used as a catalyst to control the growth position of these nanostructures. Carbon is a material with high reducing power, and the synthesis of nanostructures can be controlled by the following positional growth mechanism. The simplified chemical reaction formula is as follows:



To realize this idea experimentally, we focused on ZnO (n-type, $T_{melt} = 1975^\circ C$) and MoO_3 (n-type, $T_{melt} = 795^\circ C$) catalysts. The MO_x nanostructures, which are automatically connected to each other owing to high-density nucleation on the graphene layer, are directly applied as gas sensors, specifically for hydrogen molecules.

[†] Department of Materials Science and Engineering & Department of Energy Systems Research, Ajou University, Suwon, 16499, Republic of Korea

[†] Corresponding author: hakkiyu@ajou.ac.kr

(Received: Nov. 24, 2020, Revised: Nov. 28, 2020, Accepted: Nov. 29, 2020)

This is an Open Access article distributed under the terms of the Creative Commons Attribution Non-Commercial License (<https://creativecommons.org/licenses/by-nc/3.0/>) which permits unrestricted non-commercial use, distribution, and reproduction in any medium, provided the original work is properly cited.

2. EXPERIMENTAL

2.1 Graphene growth and transfer

Graphene was synthesized on a Cu foil through chemical vapor deposition (CVD) and transferred to a Si/SiO₂ substrate [9]. To clean and etch the surface of contaminants or native copper oxide, Cu foil (Alfa Aesar, Ward Hill, MA, USA, item no. 13382, 99.8% purity) was first immersed in 0.1 M ammonium persulfate (NH₄)₂S₂O₈ solution (Sigma-Aldrich, St. Louis, MO, USA, item no. 248614, ACS reagent, 98.0%) for 1 min. Then, it was rinsed with deionized water. The etched Cu foil was loaded into a quartz tube with a base pressure of $\sim 10^{-3}$ Torr. Heat treatment was conducted at 1000°C (heating speed: 16.67°C/min) with a H₂ gas flow of 40 sccm. CH₄ gas was introduced into the tube at 10 sccm for 10 min. The tube was rapidly cooled to room temperature to precipitate the graphene on the catalyst surface under a H₂ gas flow of 40 sccm.

2.2 Metal oxide growth

Two different MO_x powder sources were used for carbothermal transport: ZnO (Sigma-Aldrich, item No. 96479) and MoO₃ (Sigma-Aldrich, item No. M0753). The MO_x powder was mixed with graphite powder (99%, Daejung, item No. 4071-1400) at an atomic ratio of 1:2, and placed at the center of quartz tubes with alumina boats. The substrates (half of the SiO₂ surface was covered with graphene) were placed at the end of a furnace 15 cm away from the boat (see Fig. 1). The vacuum pressure was reduced to 5 mTorr using a mechanical pump. Helium gas (He) was introduced into the tube at a flow rate of 40 sccm while heating for 1 h until the growth temperature was reached. The alumina boats with the source materials were heated at the center of the furnace to 900–1000°C (ZnO) and 600°C (MoO₃). After

reaching the growth temperature, O₂ gas was introduced into the chamber for 10 min, and the flow rate was controlled within the range of 20–150 sccm for growth of the MO_x nanostructures. Afterward, the furnace was cooled to room temperature under a flow of 40 sccm.

2.3 Analysis

Raman spectra were obtained with a LabRAM HR Evolution–Nicolet iS50 (HORIBA–Thermo, Jobin Yvon) spectrometer using a He-Ne excitation source (532 nm), with a laser beam spot size of 1 μm in diameter, and an accumulation time of 60 s. X-ray diffraction was performed with a Rigaku MiniFlex spectrometer (XRD; 3 kW, Cu-Kα, HD307172) at a scan speed of 2°/min. Scanning electron microscopy (SEM) images were acquired. Hydrogen gas sensing tests were conducted using a Keithley-4200 instrument in a vacuum probe station chamber at room temperature for ZnO, and at 200°C for MoO₃. Owing to the high density of MO_x nanostructures, direct electrical wiring on the MO_x surface was done by silver paste (ELCOAT P-100, CANS) without an additional process. The distance between the electrodes was 0.5 cm.

3. RESULTS AND DISCUSSIONS

To verify the reducing power of graphene, a CVD deposition experiment was conducted using V₂O₅ powder of the V-O system. The synthesized graphene was transferred to a SiO₂ substrate (Fig. 2a) and Raman spectral analysis was performed. It can be seen that one layer of graphene was synthesized at a G/2D ratio (Fig. 2b). Then, 0.8 g of V₂O₅ powder was loaded in the cleaned alumina boat, and the substrate was placed in reverse on the alumina boat. The alumina boat with V₂O₅ powder was loaded in

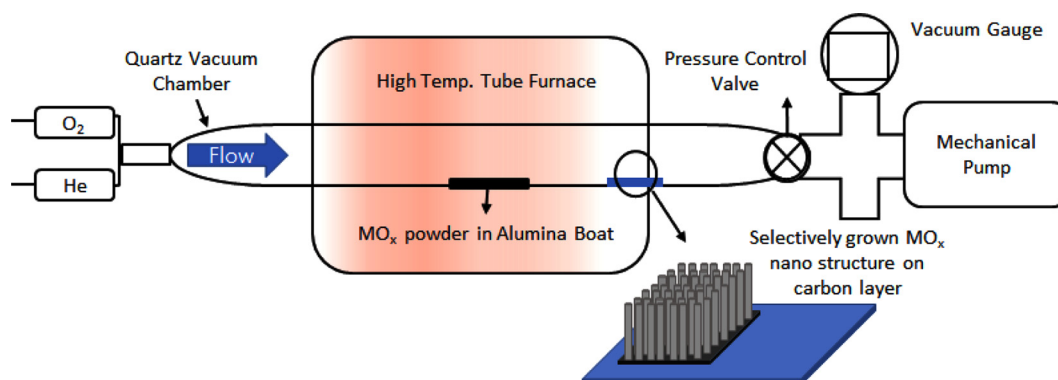


Fig. 1. Schematic image of graphene synthesized by CVD and MO_x growth.

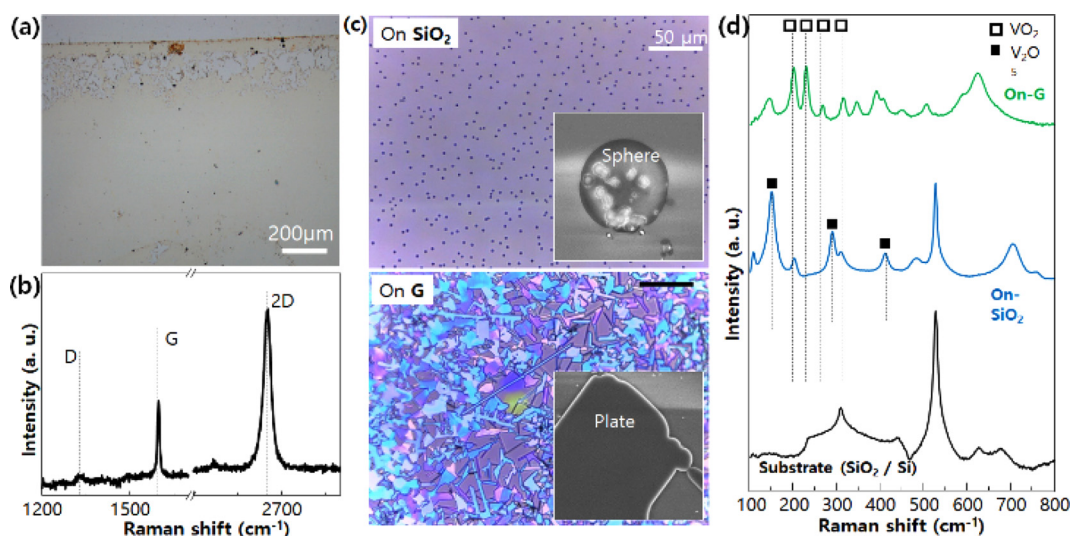


Fig. 2. (a) Digital camera image of graphene transferred on Si substrate. (b) Raman spectra of each layer of graphene. (c) OM and SEM images of vanadium oxides grown on SiO₂ and graphene. (d) Raman spectra of various shapes (sphere on SiO₂ and plane on graphene) of vanadium oxides.

a quartz tube with a base pressure of $\sim 10^{-3}$ Torr. Heat treatment was conducted at 700°C (heating speed of 17.5°C/min) with a He gas flow of 250 sccm.

Depending on the presence or absence of a graphene layer, the image after synthesis on an optical microscope varied (Fig. 2c). Spherical particles formed on the SiO₂ surface without graphene, while plate-shaped structures formed in the region to which

graphene was transferred. Raman spectral analysis (Fig. 2d) confirmed that the spherical particles were V₂O₅, and the plate-shaped structure was VO₂. Through this, the reducing power of the graphene layer can be verified [10].

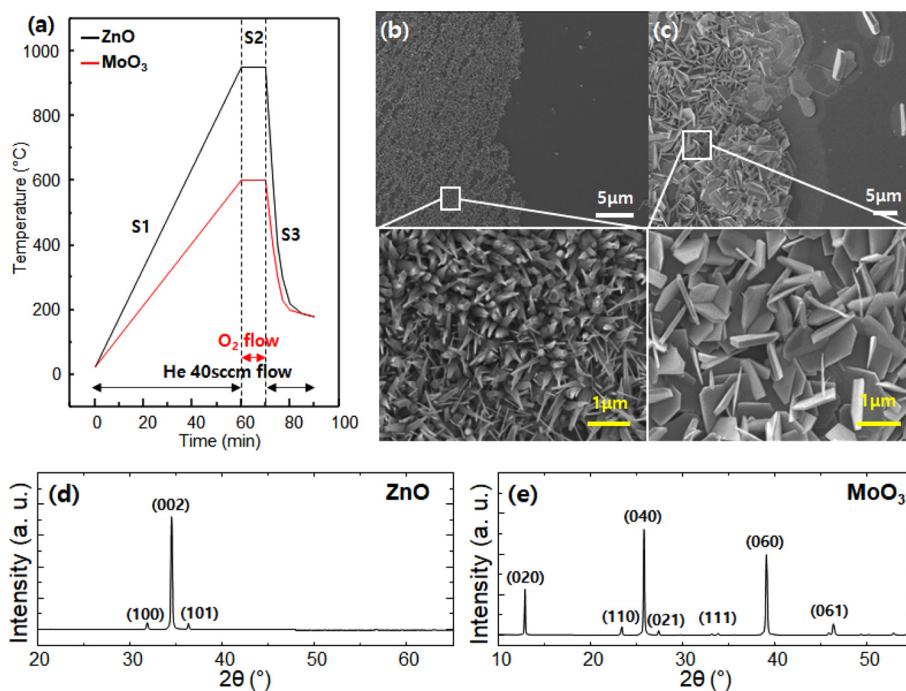
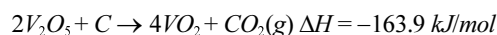


Fig. 3. (a) Time vs. temperature graph for the MO_x nanostructure growth. SEM images of MO_x grown on half of SiO₂/Si(100) substrates covered by transferred graphene: (b) ZnO grown at 970 °C; and (c) MoO₃ grown at 600°C. XRD patterns of MO_x nanostructures grown on graphene/SiO₂/Si (100): (d) ZnO and (e) MoO₃.

Based on the reducing power of graphene, an experiment on the synthesis of nanostructures was conducted by considering the melting point of ZnO and MoO₃ metal oxides (Fig. 3a). The boundaries of MO_x grown between the graphene and SiO₂ surfaces were easily distinguished (left: on graphene, right: on SiO₂) because of the low nucleation of metallic MO_x on the SiO₂ surface compared with the graphene surface (Figs. 3b and 3c). After the nucleation process, the MO_x nanostructures were developed by the anisotropic polarity between crystal orientations (rod-type for ZnO and plate-type for MoO₃). The crystallinity of the MO_x nanostructures was confirmed by XRD. The XRD profile of wurtzite ZnO (Fig. 3d) shows that it predominantly adopts the (002) preferred orientation because the hexagonal structure of graphene can act as a buffer layer and reduce the lattice mismatch. MoO₃ (orthorhombic crystal structure, $a = 3.9628 \text{ \AA}$, $b = 13.855 \text{ \AA}$, and $c = 3.6964 \text{ \AA}$) was grown on graphene with partially vertical and rectangular nanodisk shapes (Fig. 3e) because of the relatively long lattice constant of b , resulting in a high-order diffraction profile with (020), (040), and (060) peaks. The vertically connected nanodisk MoO₃ with high density may have a large surface-to-volume ratio and exhibit higher surface sensitivity than bulk films.

To confirm the effects of changing the arrangement and shape

of the formed nanostructure bundles on the performance of the hydrogen sensor, the experiment was conducted by controlling the oxygen partial pressure in the case of ZnO. At a low oxygen flow rate, the synthesized ZnO nanostructures were randomly distributed and branched (Fig. 4a). On the other hand, at a high oxygen flow rate, the ZnO nanostructures had a vertical hexagonal shape, as shown in Fig. 4b. At a low oxygen flow rate (20 sccm), the nanostructures were grown by the vapor–liquid–solid growth mechanism. The evaporated Zn atoms were insufficiently oxidized, leading to additional metallic nucleation on the graphene surface and the side wall of the pre-grown ZnO with random orientation (Fig. 4c). At a high oxygen flow rate (150 sccm), the vapor–solid growth mechanism was dominant because the Zn atoms that evaporated during the carbothermal reaction quickly reacted with sufficient oxygen, and a high flux of ZnO vapor was solidified on graphene with a (002) preferred orientation (Fig. 4d).

High-density MO_x nanostructures with a large surface-to-volume ratio can be applied in hydrogen gas sensors. Fig. 5 shows the change in the resistance of the gas sensors fabricated using the MO_x nanostructures (ZnO and MoO₃) with respect to the on/off switching of 10% hydrogen gas diluted with nitrogen gas at a fixed DC voltage of 1 V. The ZnO- and MoO₃-based sensors showed fast on/off switching characteristics resulting from typical

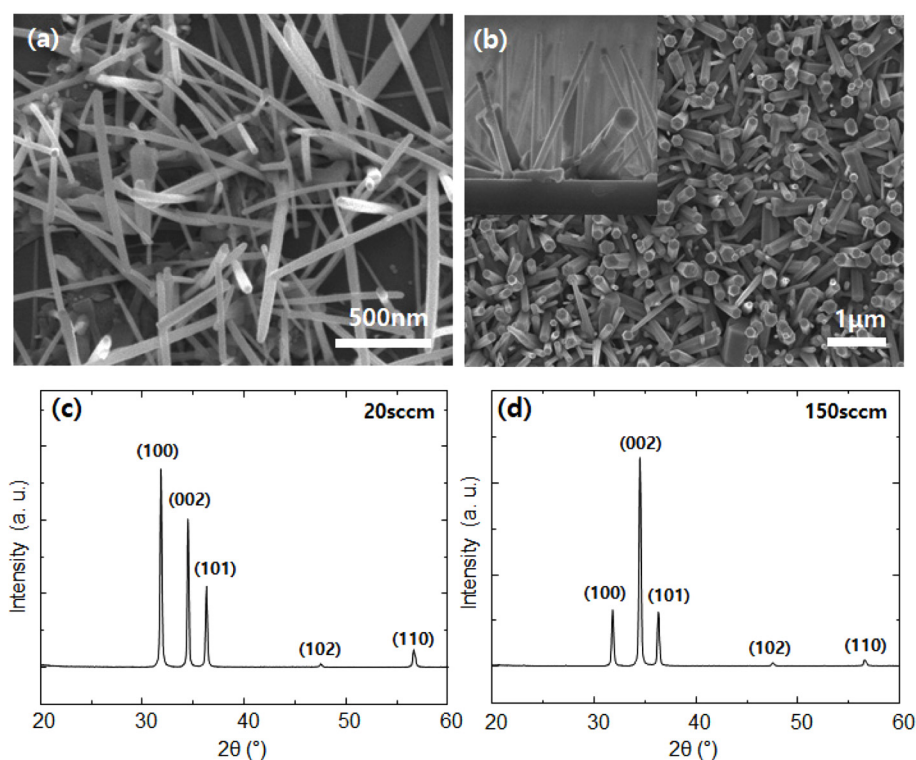


Fig. 4. (a, c) SEM images and XRD patterns of ZnO nanostructures grown at 1000°C under 20 sccm oxygen flow rate. (b, d) Top-view and cross-sectional (inset) SEM images and XRD patterns of ZnO nanorods grown at 1000°C under 150 sccm oxygen flow rate.

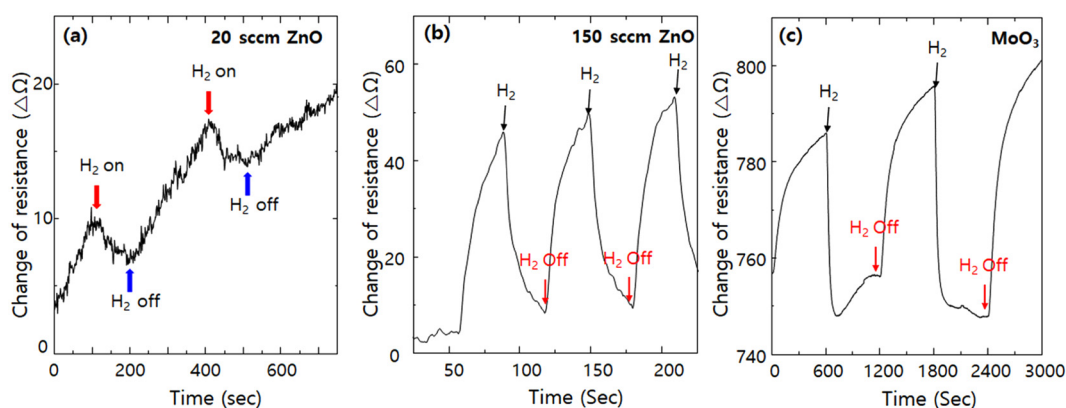


Fig. 5. H₂ (10% diluted with nitrogen gas) sensing tests (a, b) employing ZnO at room temperature, and (c) MoO₃ at 200°C.

n-type surface semiconductor gas sensors. Specifically, in the case of ZnO, depending on the growth conditions, the injection of 150 sccm of oxygen yielded better sensor characteristics compared with the injection of 20 sccm of oxygen. This is attributed to insufficient oxidation and the increase in the ratio of metallic Zn to ZnO.

4. CONCLUSIONS

In summary, the thermal transport growth of various MO_x nanostructures using graphene as a catalytic layer was studied. The sp²-bonded carbon atoms of graphene readily formed metal-carbide bonds, resulting in the preferred nucleation of MO_x on the transferred graphene area. By using this experimental protocol, the position of the MO_x nanostructures as well as the growth parameters, such as nucleation density and growth rate, were controlled. The position-selective and density-controlled MO_x nanostructures were evaluated for hydrogen gas sensors. The ZnO and MoO₃ nanostructures exhibited the typical behavior of n-type semiconductor gas sensors with stable sensitivity. We believe that the graphene catalytic layer can be applied in various fields and devices that employ the growth of functional MO_x nanostructures.

ACKNOWLEDGMENT

This research was supported by the Basic Science Research Program through the National Research Foundation of Korea (NRF), funded by the Ministry of Science, ICT & Future Planning (NRF-2019R1A2C1006972).

REFERENCES

- [1] K. J. Choi and H. W. Jang, "One-Dimensional Oxide Nanostructures as Gas-Sensing Materials: Review and Issues", *Sensors*, Vol. 10, pp.4083-4099, 2010.
- [2] Z. Zhao, M. A. Carpenter, H. Xia, and D. Welch, "All-optical hydrogen sensor based on a high alloy content palladium thin film", *Sens. Actuator B*, Vol. 113, pp.532-538, 2006.
- [3] X. H. Chen and M. Moskovits, "Observing catalysis through the agency of the participating electrons: Surface-chemistry-induced current changes in a tin oxide nanowire decorated with silver", *Nano Lett.*, Vol. 7, pp.807-812, 2007.
- [4] H. T. Wang, B. S. Kang, F. Ren, L. C. Tien, P. W. Sadik, D. P. Norton, S. J. Pearton, and J. S. Lin, "Hydrogen-selective sensing at room temperature with ZnO nanorods", *Appl. Phys. Lett.*, Vol. 86, pp.243503(1)-243503(3), 2005.
- [5] U. T. Nakate, R. Ahmad, P. Patil, Y. T. Yu, and Y. B. Hahn, "Ultra thin NiO nanosheets for high performance hydrogen gas sensor device", *Appl. Surf. Sci.*, Vol. 506, pp.144971(1)-144971(8), 2020.
- [6] Y. Wang, B. Liu, D. Cai, H. Li, Y. Liu, D. Wang, L. Wang, Q. Li, and T. Wang, "Room-temperature hydrogen sensor based on grain-boundary controlled Pt decorated In₂O₃ nanocubes", *Sens. Actuator B*, Vol. 201, pp.351-359, 2014.
- [7] S. Aygün and D. Cann, "Hydrogen sensitivity of doped CuO/ZnO heterocontact sensors", *Sens. Actuator B*, Vol. 106, pp.837-842, 2005.
- [8] X. Hu, J. C. Yu, J. Gong, Q. Li, and G. Li, "α-Fe₂O₃ Nanorings Prepared by a Microwave-Assisted Hydrothermal Process and Their Sensing Properties", *Adv. Mater.*, Vol. 19, pp.2324-2329, 2007.
- [9] H. K. Yu, "Effective reduction of copper surface for clean graphene growth", *J. Electrochem. Soc.*, Vol. 162, pp. E277-E281, 2015.
- [10] H. J. Lee, U. J. Yang, K. N. Kim, S. Park, K. H. Kil, J. S. Kim, A. M. Wodtke, W. J. Choi, M. H. Kim, and J. M. Baik, "Directional Ostwald ripening for producing aligned arrays of nanowires", *Nano Lett.*, Vol. 19, pp.4306-4313, 2019.